Hindawi
Advances in Materials Science and Engineering
Volume 2022, Article ID 6048588, 17 pages
https://doi.org/10.1155/2022/6048588

Research Article

An Investigation on the Influences of Construction Schemes on Backfilling the River-Crossing Section of a Utility Tunnel

Jin-Kun Huang,[1,2] **Zhao-Xiang Lu**,[1] **Wan-Yun Yin**,[1] **Ren-Cai Jin**,[1] **Yuan-Di Qian**,[1,3] **Si-Dong Shen**,[4] **and Lei Wang**[4]

[1]*China MCC17 Group Co. LTD, Maanshan, Anhui 243000, China*
[2]*School of Naval Architecture, Ocean and Civil Engineering, Shanghai Jiao Tong University, Shanghai 200240, China*
[3]*Department of Civil Engineering and Architecture, Anhui University of Technology, Maanshan, Anhui 243000, China*
[4]*School of Urban Railway Transportation, Shanghai University of Engineering Science, Shanghai 201620, China*

Correspondence should be addressed to Jin-Kun Huang; jkunhuang@sjtu.edu.cn

Received 22 February 2022; Revised 9 August 2022; Accepted 27 September 2022; Published 7 November 2022

Academic Editor: Antonio Boccaccio

The backfill construction of a utility tunnel is as important as its main structure construction. While the existing research on utility tunnels focuses on the construction of the main structure, rare attention has been paid to the backfill construction. In this paper, with a practical comprehensive utility tunnel project as the background, a variety of different backfill construction schemes were designed, and the corresponding numerical simulations were performed with the finite element analysis software Midas. The influence of different backfill construction schemes on the side wall, roof, and floor of the utility tunnel was systematically studied and analyzed, and the displacement and stress variation curves in the process of utility tunnel backfill were obtained. Based on the simulation results and the actual engineering situation, the optimal schemes for utility tunnel backfill construction were determined. The results show that the displacement of the side wall of the utility tunnel increased first and then decreased with increasing backfill soil in the unilateral backfill mode, and there was little displacement in the bilateral backfill mode. The shear stress of the side wall of the utility tunnel in both the unilateral and bilateral backfill modes gradually increased with the backfill process. Within the region 1 m above the roof of the utility tunnel, backfill modes had no effect on the final stress and displacement values, but the layering method made a difference. Accordingly, bilateral backfill mode is suggested for the region below the roof of the utility tunnel, while in the case of region 1 m above the roof, backfilling is recommended to be layered according to height rather than position.

1. Introduction

Urban underground utility tunnels, also known as the common ditches, scientifically compartmentalize municipal pipelines such as electricity, water supply and drainage, communication, and gas pipelines in one single tunnel. It is well known that the construction of an underground utility tunnel can not only make full use of underground space, improve the quality of safe operation, the ability of disaster prevention and relief, and traffic conditions, create a harmonious ecological environment, and realize the sustainable development of the city, but also optimize the layout and form of urbanization, promoting quality new urbanization in China. Therefore, to efficiently build a quality utility tunnel is very significant to urban development.

The construction scheme is the key to such concern because of the consolidation process, stress release, and other factors [1–3]. Scientific and reasonable selection of a construction scheme can not only ensure quality, safe, and cost-efficient construction of a project but also reduce total social investment, optimize industrial structure, and promote urbanization construction [4, 5]. In this regard, a lot of research has been conducted on the construction of utility tunnels. Hu and Zhang [6] established an integrated design

and construction optimization model based on Building Information Modeling (BIM) technology in order to improve the efficiency of the design and construction of the conventional utility tunnel. Zheng and Shicheng [7] have researched the modeling and application of BIM-based tunnel technology. Liu et al. [8] conducted a numerical analysis using the Fast Lagrangian Analysis of Continua 3D (FLAC3D) to investigate the effect of different construction options on tunnel uplift as well as the effect of factors such as excavation sequence and depth of ground reinforcement on tunnel uplift. Morovatdar et al.'s [9] research found that the pre-excavation deployment of the Umbrella Arch Method (UAM) can significantly reduce the settlement of the tunnel crown and ground surface. Zhao et al. [10] optimized the construction parameters and identified engineering measures to stabilize the tunnel face in order to ensure the safe and rapid construction of the large section of loess tunnel. Li et al.'s[11] research found that the use of noncircular tunnel-boring machines (TBMs) has great advantages in terms of construction schedules, settlement control, and space utilization. Chen et al. [12] give a method for calculating the temperature field in tunnels using three-dimensional finite elements for freezing tunnel construction. Lu et al. [13] had proposed a steel-supported cut pipe method (SSCP) that improves construction safety and the utilization of underground space. Miao et al. [14] studied the mechanical properties and optimal design of the soil mixing wall (SMW) construction method piles (reinforced cement mixing piles) in water-rich soft ground in integrated pipe corridors.

In addition, there are several studies on the backfill construction of a utility tunnel. Che et al. [15] studied the relationship between stress and strain changes in the corrugated steel utility tunnel (CSUT) during tunnel backfilling. Sun et al. [16] used the three-dimensional finite element model to explore the influence of the longwall panel width, advancing distance, and backfill-material's compaction ratio (BMCR) on the deformation characteristics of the porous tunnel in order to study the influence of coal mining on the stability of the overlying porous tunnel. Wang et al. [17] used the finite element software FLAC3D for numerical analysis to prove the rationality of backfill parameters and the effectiveness of support under the influence of groundwater when the tunnel passes through a large karst cave. To cope with the backfill-material problems existing in backfilling the foundation pit of the utility tunnel, Yao et al. [18] developed the method of mixing cement and other additives in the excavation soil, forming a kind of environmentally friendly self-compacting cement-soil backfill-material characterised by high fluidity, strength, and impermeability.

In summary, the selection of the construction scheme of an urban underground utility tunnel is very important. However, relevant research focuses on the construction of the construction of the main structure of the utility tunnel, with several studies about backfill material. Investigations into the backfilling construction schemes are rather limited. Therefore, in the present study, a section of the utility tunnel beneath the Gaochao River in Ma'anshan was taken as the background. Based on the existing conditions, backfill construction schemes embracing four operational modes and two cases were designed and simulated with the finite element software Midas GTS NX. Then, the influences of different backfill construction schemes on the side wall, roof, and floor of the utility tunnel were systematically studied, with the corresponding variation laws of displacement and stress in the backfill process obtained. Finally, based on the numerical simulation results, two optimal backfill construction schemes were determined. It provides references and guidance for the selection of backfill construction schemes for similar projects.

2. Backfill Construction Technology for the River-Crossing Sections of Utility Tunnels

The construction of urban underground utility tunnels is usually accompanied by the construction of new roads, which is the so-called "tunnel-below-road-above" mode. In this case, the compactness of the backfill needs to be greater than 0.90, and the new and old soil layers must be closely integrated. Otherwise, roads will be prone to uneven settlement, incurring the risk of large-scale rework. According to the Chinese National Standard (GB50838-2015), artificially layered backfill compaction is required on both sides of the utility tunnel and within the region 1 m above its roof. However, in practice, due to the large dimension of the utility tunnel construction, the backfill workload often tends to be very large. Particularly, for positions with foundation pit supports such as steel sheet piles and soil nailing walls, the steel sheet piles and the spraying anchors of the soil nailing walls need to be removed in advance, which further prolongs the construction cycle and poses a threat to safety. Apparently, the prescription is too demanding to be met with current construction methods.

To address such issues, a new backfill construction method for utility tunnels will be illustrated in this section, which features by large-scale mechanical backfill and subsequent compaction grouting treatment.

2.1. Technological Process Flow. The technological process flow is the core of engineering construction. The backfill construction process is shown in Figure 1.

2.2. Operational Key Points

(1) Cleaning of the foundation pit of the utility tunnel: before backfilling, the main body and waterproof structure of the utility tunnel should pass the acceptance. Construction waste and water beside the site should be cleaned up, and backfilling construction can only begin with written consent from the owner and the supervisor.

(2) Removal of the original foundation pit supports: before backfilling, the original foundation pit supports should be removed, and the spraying surface of reinforcement mesh should be eradicated with an excavator.

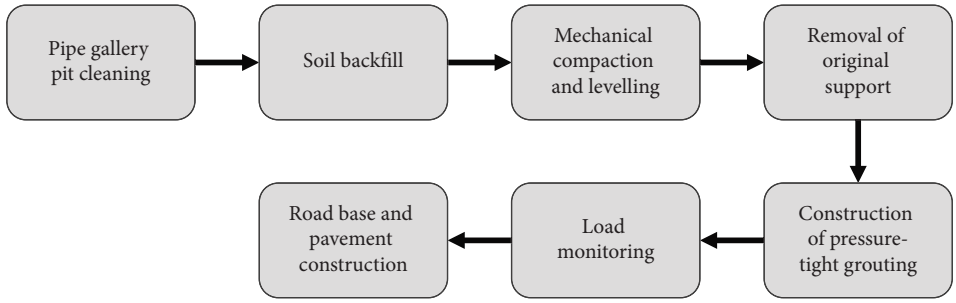

Figure 1: Proposed backfill construction process.

(3) Backfilling: after the support structures have been removed, an excavator or a loader is used to mechanically backfill on both sides of the utility tunnel. The backfill region covers both sides of the utility tunnel and is 1 m above its roof. Figure 2 shows the concrete backfill process.

(4) Mechanical compaction and grading: after the backfilling, the soil surface should be leveled and rolled using loaders and presses.

(5) Compaction grouting construction: the pile-position line should be arranged on both sides of the utility tunnel. The compaction grouting region should include both the old and new soil layers, and the grouting depth should be greater than 1 m above the utility tunnel. The grouting pressure should be controlled within 0.3–0.5 MPa in the region beside the tunnel and below the floor, and within 0.6–0.8 MPa in the region from the roof to the bottom of the road base. According to the characteristics of the channel of the Gaochao River, the grouting pressure was determined to be 0.4 MPa after a field test.

(6) Bearing capacity tests for backfill: according to GB50838-2015, a compaction test should be conducted after each layer of backfilling during the backfilling process of the utility tunnel. Yet because the present construction process backfills once and for all, layer-by-layer compaction tests were infeasible. Instead, the post-treatment bearing capacity of the soil on both sides of the utility tunnel was tested by way of the foundation case. After meeting the requirements, it is handed over to the next process of construction.

(7) Construction of the subgrade and pavement.

(8) River embankment restoration on both sides.

(9) Removal of the drainage pipe and cofferdam.

The construction scheme of this project (the river-crossing section of the utility tunnel) is shown in Figure 3.

3. Designed Backfill Construction Scheme of the Utility Tunnel and Its Optimization

The backfill construction is divided into two regions, including the region on both sides below the roof of the utility tunnel (region 1) and that above 1 m above the roof of the utility tunnel (region 2). Region 1 can be backfilled in unilateral or bilateral backfill mode, while region 2 can adopt the left-to-right (or right-to-left) or middle-to-side mode. As for region 2, each mode can be further separated into two cases, with Case I giving priority to backfilling by position and Case II by height. The concrete backfill construction scheme is shown in Figure 4 and Table 1.

4. Numerical Simulations of the Backfill Construction of the River-Crossing Section of the Utility Tunnel

4.1. Model Introduction. Figures 5 and 6 show the river-crossing section of the utility tunnel and its two-dimensional model established by Midas GTS NX, respectively. Accordingly, the depth of the river above the excavation section of the foundation pit is about 2.5 m, and the depth of the foundation pit in the standard section is 7.2 m, which means it is a deep foundation pit. The upper opening of the foundation pit is 28 m, and the bottom width is 11.5 m. The slope steps beside the foundation pit are 1 m wide, with a slope coefficient equal to 1. The side wall of the utility tunnel is 3.8 m high, and the width of the floor as well as the roof is 7.5 m. The utility tunnel has two rectangular cabins, each of which is 3 m high and 3.25 m wide.

With regard to the boundary conditions of the model, both sides were constrained in the normal direction, with the bottom fixed and the top free. The model was discretized by 10-node high-order tetrahedral elements, totaling 2330 elements and 9210 nodes. As for the choice of constitutive models, the main structure of the utility tunnel, made of concrete, was regarded as linear-elastic, while the backfill was assumed to follow the Mohr-Coulomb constitutive model. Because the original soil was not qualified for backfilling, a new grouting construction method for utility tunnel backfill was proposed, i.e., after backfilling the utility tunnel with the original soil, the backfill soil and the undisturbed soil around the utility tunnel were compacted and grouted so that they were closely combined and the strength parameters of the soil were improved. The improved parameters, listed in Table 2, are then adopted in the present simulations.

4.2. Simulated Conditions of the Utility Tunnel Backfill Process

4.2.1. Unilateral Backfilling in Region 1. Due to symmetry, there is no difference between the left-to-right and right-to-

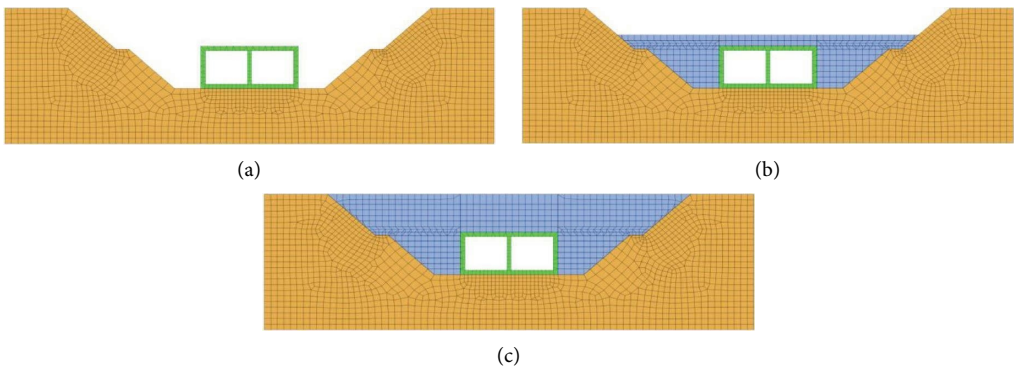

Figure 2: Backfill process. (a) Before backfilling of the integrated pipe corridor. (b) After backfilling of the integrated pipe corridor. (c) After backfilling of the integrated pipe corridor pit.

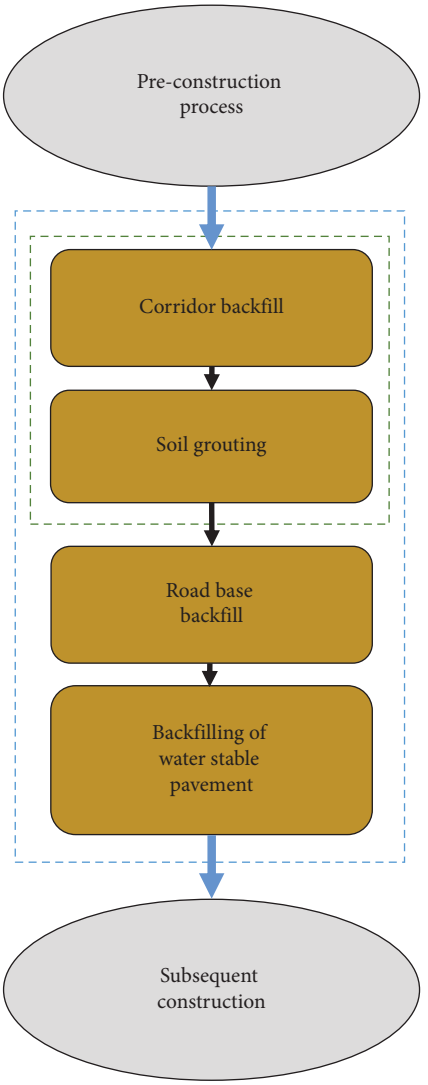

Figure 3: Construction scheme for the river-crossing section of the utility tunnel.

left orders in the unilateral backfill process. Therefore, the backfill analysis in this section was based on the left-to-right order, and the concrete backfill process is shown in Figure 7.

(1) Initial stress balance, denoted as *S*0

(2) The backfill height of the left side reached 0.5 m, denoted as *S*1

(3) The backfill height of the left side reached 1 m, denoted as *S*2

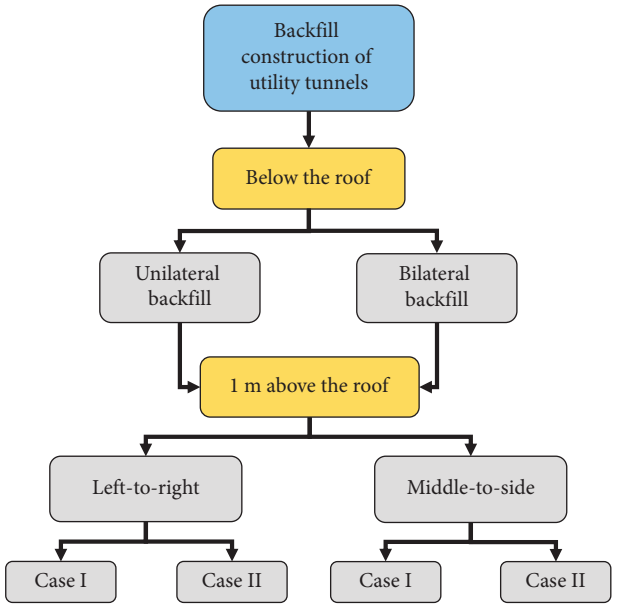

Figure 4: Diagram of backfill construction schemes for the utility tunnel.

Table 1: Designed backfill construction scheme of the utility tunnel.

Scheme	Below the roof	1 m above the roof	
1	Unilateral backfill	Left-to-right	Case I
2			Case II
3		Middle-to-side	Case I
4			Case II
5	Bilateral backfill	Left-to-right	Case I
6			Case II
7		Middle-to-side	Case I
8			Case II

Figure 5: Excavation site of the river-crossing section.

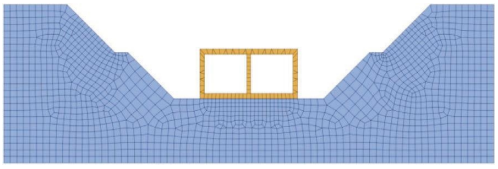

Figure 6: Two-dimensional model of the river-crossing section.

(4) The backfill height of the left side reached 1.5 m, denoted as *S*3

(5) The backfill height of the left side reached 2 m, denoted as *S*4

(6) The backfill height of the left side reached 2.5 m, denoted as *S*5

(7) The backfill height of the left side reached 3 m, denoted as *S*6

(8) The backfill height of the left side reached 3.5 m, denoted as *S*7

(9) The backfill height of the left side reached 3.8 m, denoted as *S*8

(10) Backfill on the right side of the utility tunnel (the same as that on the left side) until the backfill on the right side is flat with the roof of the utility tunnel

4.2.2. Bilateral Backfilling in Region 1. The bilateral backfilling process resembled that of unilateral mode except that the backfilling of both sides was performed simultaneously. The specific backfilling process is shown in Figure 8.

(1) Initial stress balance, denoted as *S*0

(2) The backfill height of both sides reached 0.5 m, denoted as *S*1

(3) The backfill height of both sides reached 1 m, denoted as *S*2

(4) The backfill height of both sides reached 1.5 m, denoted as *S*3

(5) The backfill height of both sides reached 2 m, denoted as *S*4

(6) The backfill height of both sides reached 2.5 m, denoted as *S*5

(7) The backfill height of both sides reached 3 m, denoted as *S*6

(8) The backfill height of both sides reached 3.5 m, denoted as *S*7

(9) The backfill height of both sides reached 3.8 m, denoted as *S*8

4.2.3. Left-to-Right Backfilling in Region 2. The Case I backfilling process is shown in Figure 9.

(1) Initial stress balance, denoted as *S*0

(2) The backfill height of the left side reached 0.5 m, denoted as *S*1

(3) The backfill height of the left side reached 1 m, denoted as *S*2

(4) The backfill height of the roof reached 0.5 m, denoted as *S*3

(5) The backfill height of the roof reached 1 m, denoted as *S*4

(6) The backfill height of the right side reached 0.5 m denoted as *S*5

(7) The backfill height of the right side reached 1 m, denoted as *S*6

The Case II backfilling process is demonstrated in Figure 10.

Table 2: Basic physical and mechanical parameters of the materials.

Materials	Density (kg/m^3)	Young's modulus (kPa)	Poisson's ratio	Cohesion (kPa)	Internal friction angle (°)
Soil	1.49	12000	0.30	21.5	20
Grouted soil	1.59	21600	0.32	28	26
Concrete	2.35	31500000	0.2	—	—

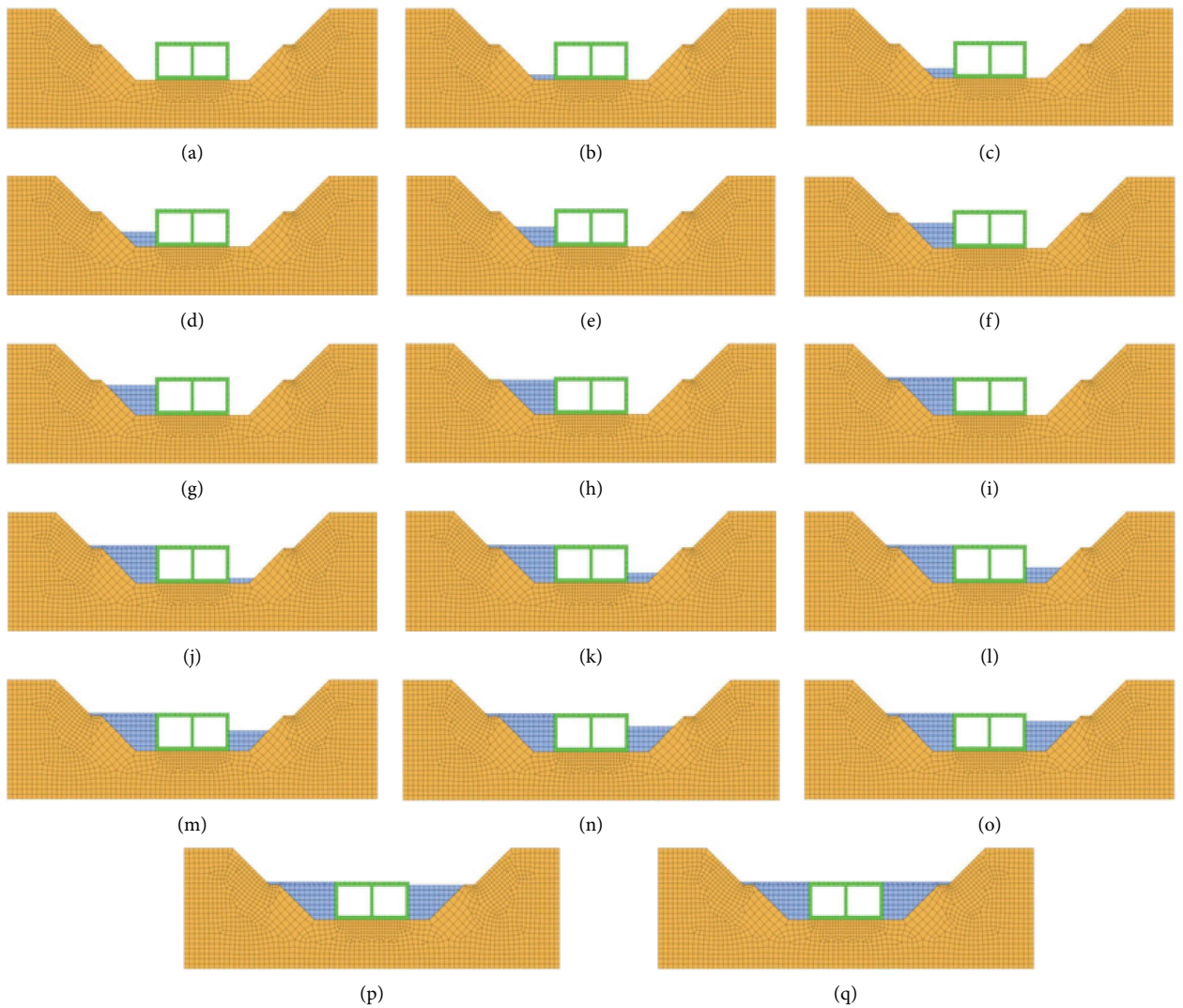

Figure 7: Unilateral backfilling in region 1.

(1) Initial stress balance, denoted as *S*0

(2) The backfill height of the left side reached 0.5 m, denoted as *S*1

(3) The backfill height of the roof reached 0.5 m, denoted as *S*2

(4) The backfill height of the right side reached 0.5 m, denoted as *S*3

(5) The backfill height of the left side reached 1 m, denoted as *S*4

(6) The backfill height of the roof reached 1 m, denoted as *S*5

(7) The backfill height of the right side reached 1 m, denoted as *S*6

4.2.4. Middle-to-Side Backfilling in Region 2. Case I backfilling process is shown in Figure 11.

(1) Initial stress balance, denoted as *S*0

(2) The backfill height of the roof reached 0.5 m, denoted as *S*1

(3) The backfill height of the roof reached 1 m, denoted as *S*2

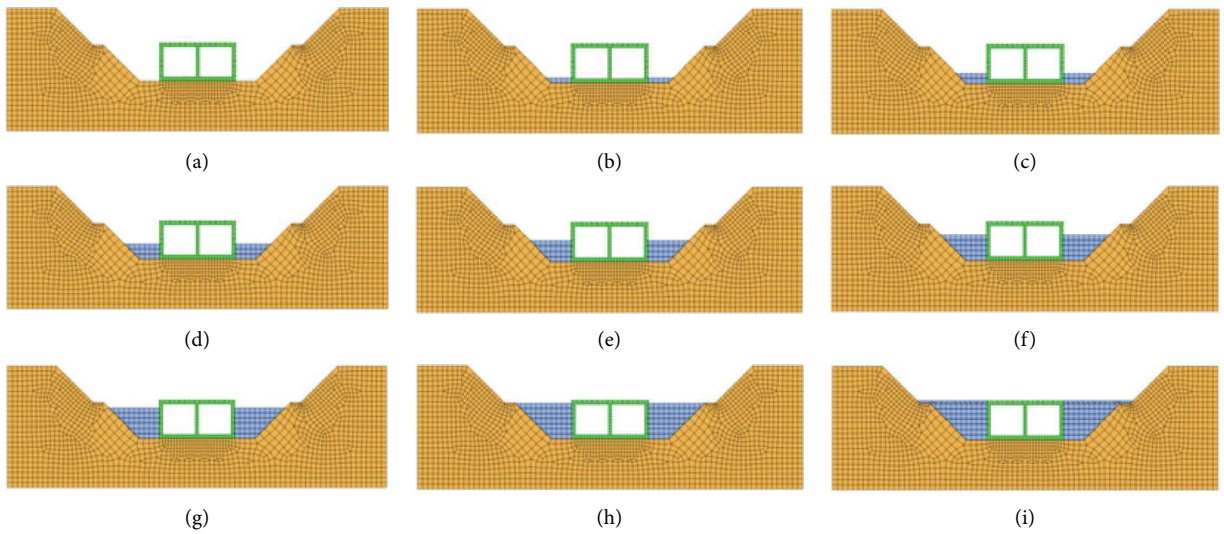

Figure 8: Bilateral backfilling in region 1.

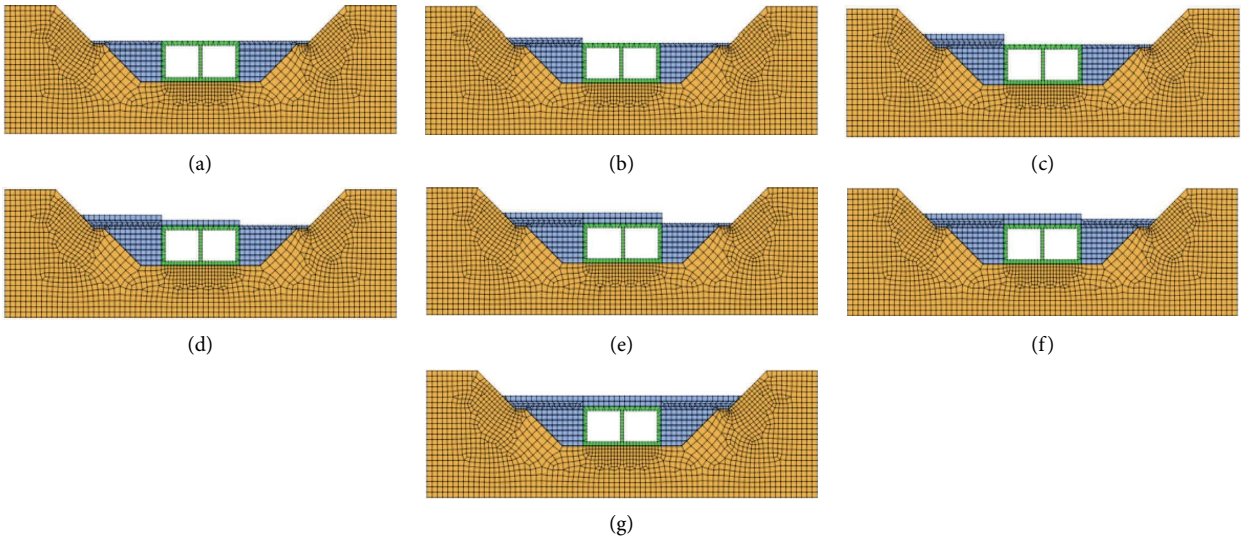

Figure 9: Backfilling from left-to-right: Case I.

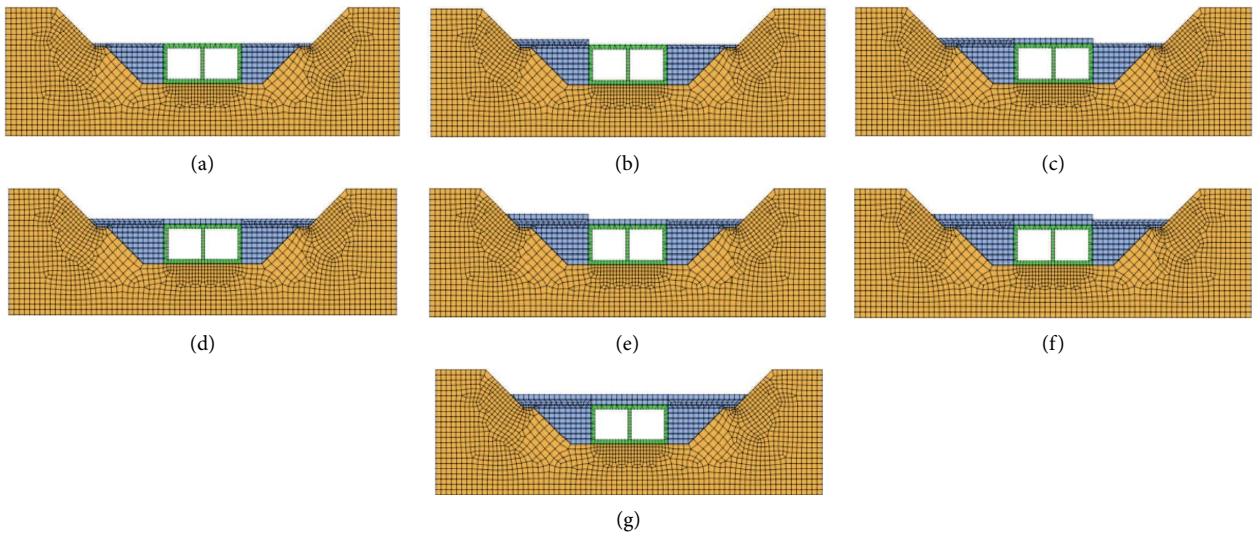

Figure 10: Backfilling from left-to-right: Case II.

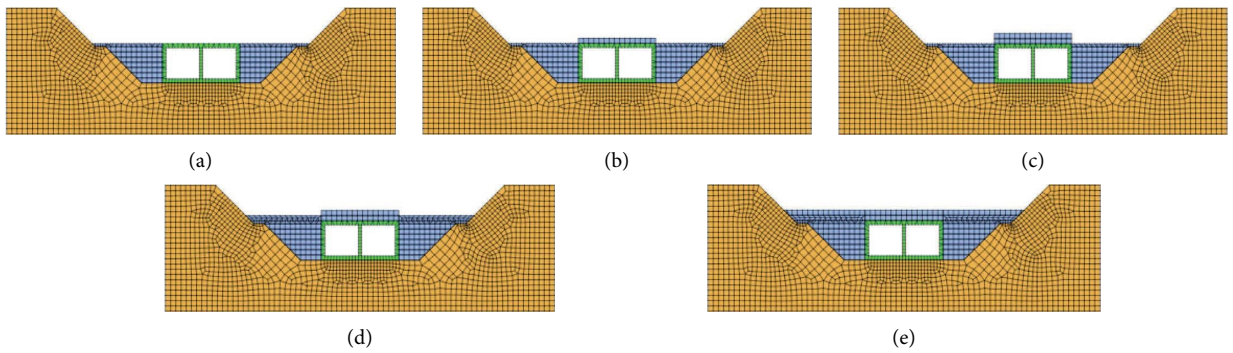

Figure 11: Backfilling from the middle to both sides: Case I.

(4) The backfill height of both sides reached 0.5 m, denoted as *S*3

(5) The backfill height of both sides reached 1 m, denoted as *S*4

Case II backfilling process is shown in Figure 12.

(1) Initial stress balance, denoted as *S*0

(2) The backfill height of the roof reached 0.5 m, denoted as *S*1

(3) The backfill height of both sides reached 0.5 m, denoted as *S*2

(4) The backfill height of the roof reached 1 m, denoted as *S*3

(5) The backfill height of both sides reached 1 m, denoted as *S*4

4.3. Simulated Conditions of the Grouting Process

(1) The initial stress balance was completed by backfilling the 1 m range on both sides of the utility tunnel and above the roof, denoted as *S*0.

(2) Utility tunnel backfill grouting completed stress analysis, denoted as *S*1; among them, the backfill grouting simulation of the utility tunnel is realized by replacing the soil strength parameters. The soil strength parameters on both sides of the utility tunnel and within a range of 1 m above the roof of the utility tunnel are replaced by grouting filling parameters.

4.4. Simulation of Subgrade and Water Stabilized Pavement

(1) The initial stress balance of the utility tunnel after grouting is denoted as *S*0.

(2) road base backfill of 1 m, denoted as *S*1.

(3) water-stable pavement backfill of 1.4 m, denoted as *S*2.

(4) excavation backfill is completed, taking into account the effect of 2.5 m water pressure on the utility tunnel across the river. The influence of water pressure is considered by applying a pressure load to the water-stabilized layer pavement, denoted as *S*3.

5. Results and Discussion

5.1. Backfilling. In this section, the analysis was performed based on the displacement and stress results of the interested positions (Figure 14) in the tunnel. Since the two regions were backfilled sequentially, the analysis was divided into two steps, too. The first step mainly focused on the variation law of displacement and shear stress in the x direction of the side walls of the utility tunnel after region 1 was backfilled, while the second step focused on the change law of Y-direction displacement and stress of the roof and floor after region 2 was backfilled.

5.1.1. Influences of Unilateral and Bilateral Backfilling Modes. Figure 15 represents the variation of lateral wall displacement in the X direction in unilateral and bilateral backfill modes, respectively, where Dx-L and Dx-R denote the values read at position x of the left wall and right wall in the unilateral backfill mode, respectively, and Sx-L and Sx-R in the bilateral backfill mode, respectively. It can be seen from Figure 15 that in the process of bilateral backfill, the lateral wall's displacement is negligible, while in the process of unilateral backfill, the displacement of the side wall initially increased and then decreased with the backfill construction, and the maximum displacement always appeared at stage four of the backfill construction. The main reason for this change is that the soil on both sides of the utility tunnel was the same in the bilateral backfill, and the soil's action on the side wall is consistent. Hence, the bilateral backfill will not produce a sliding trend, and the displacement is zero. In the unilateral backfill mode, the earthwork on the left side kept increasing before stage four, while the backfill on the right side of the utility tunnel began after the completion of the left backfill, so the displacement of the side wall of the utility tunnel increased first and then decreased. In addition, it can be seen from Figure 15 that the displacement of position 1 of the walls on both sides was always positive in unilateral mode, while the displacements of the other positions were always negative, and the farther away from position 1, the more negative the displacement was. This phenomenon is attributed to the fact that, with the progress of backfill

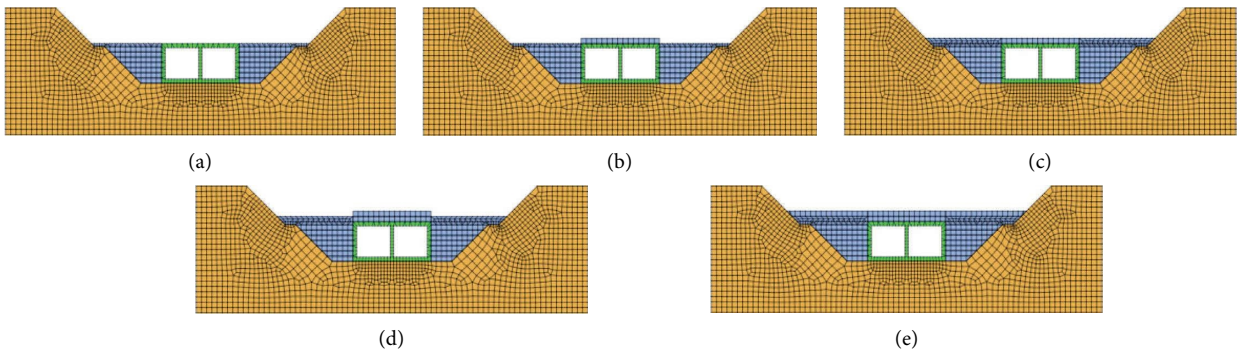

Figure 12: Backfilling from middle to both sides: Case II.

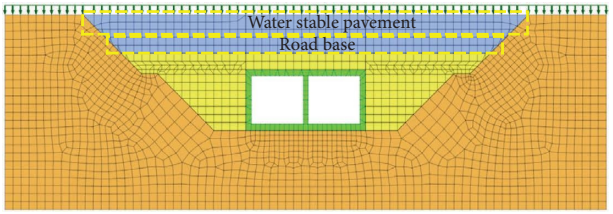

Figure 13: Diagram of the subgrade and water-stable layer.

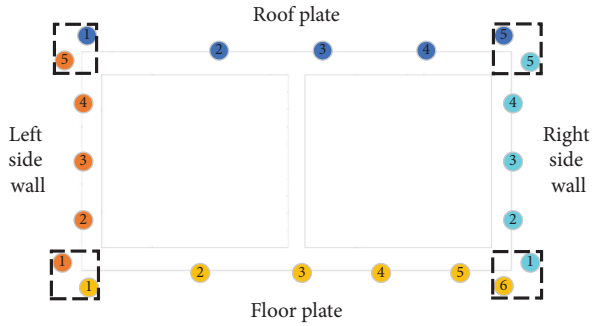

Figure 14: Interested positions in the utility tunnel.

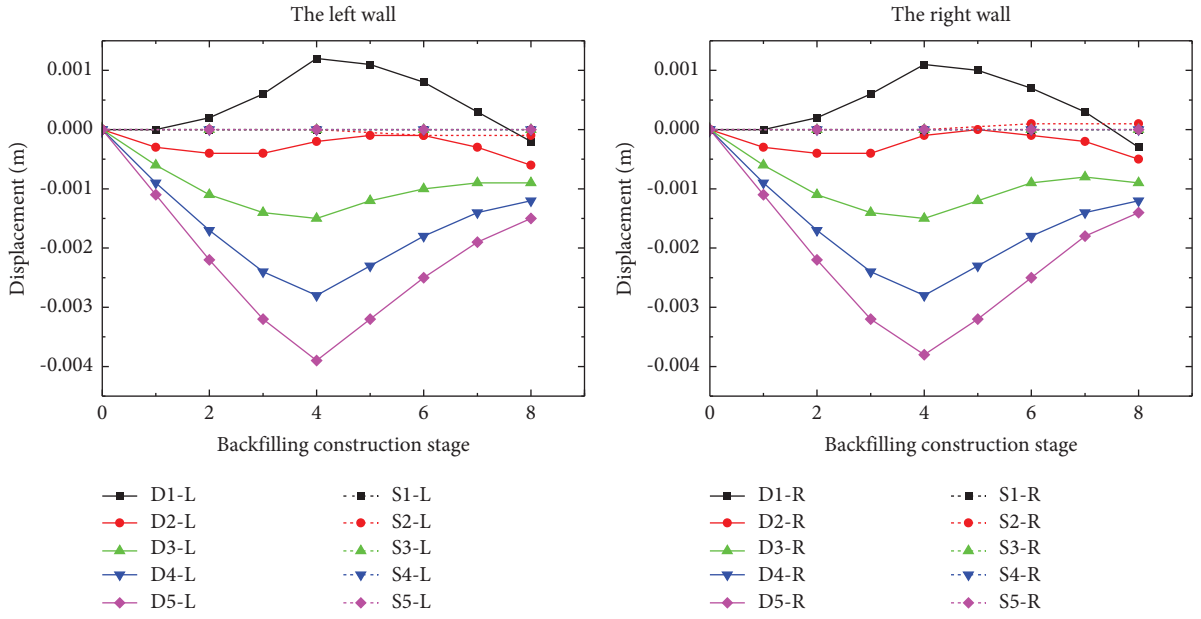

Figure 15: (X)-direction virtual displacement of the left/right wall in unilateral and bilateral backfill modes, respectively.

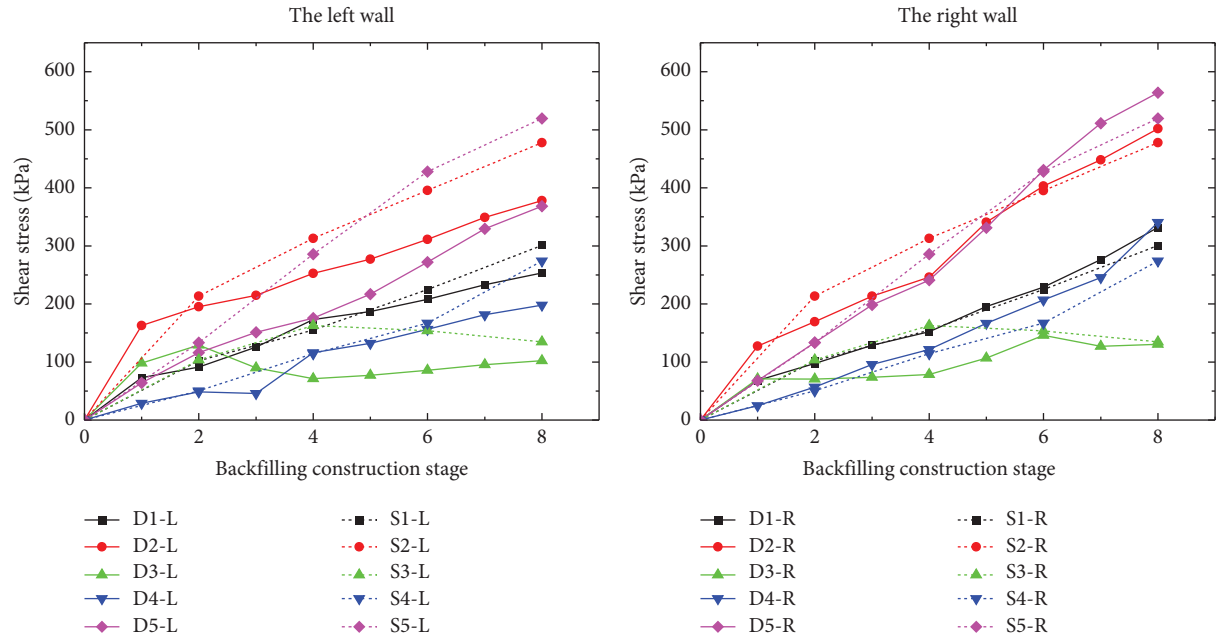

Figure 16: Shear stress of the left/right wall in unilateral and bilateral backfill modes, respectively.

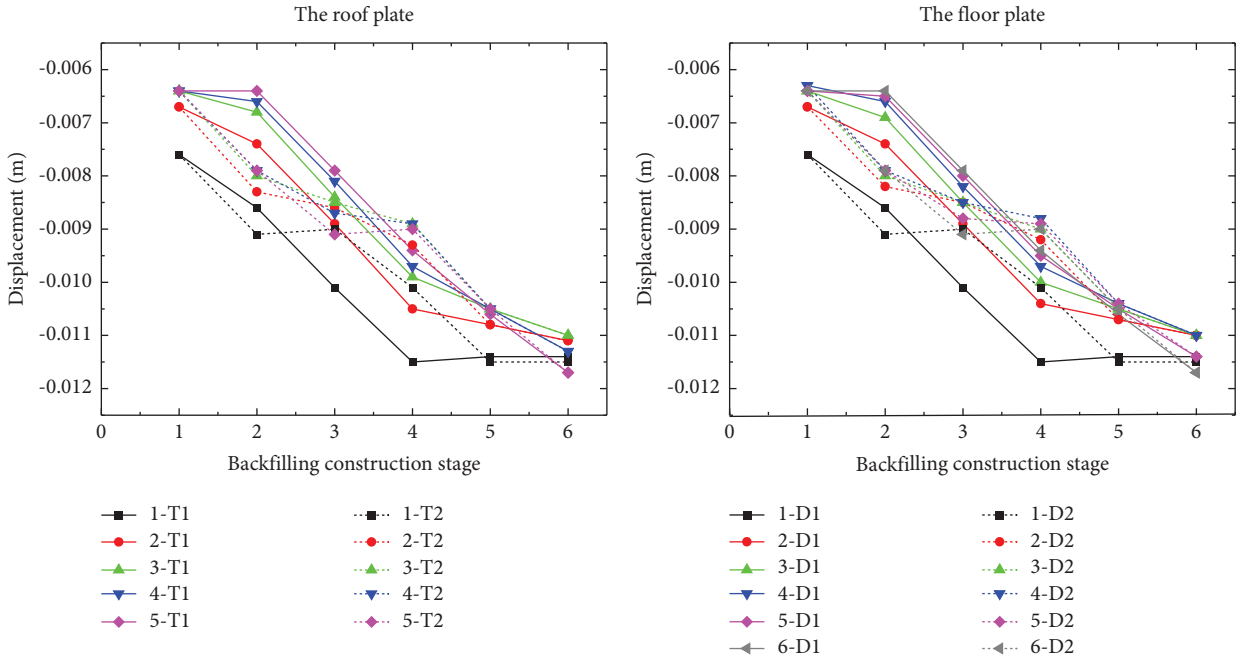

Figure 17: (Y)-direction virtual displacement of the roof/floor in the left-to-right backfilling mode.

construction, the center of gravity of backfill soil on both sides continued to move upwards, and the center of gravity was always above position 1 of the side wall. The farther away from position 1, the larger the displacement radian would be.

Figure 16 shows the variation law of shear stress on side walls in the unilateral and bilateral backfill modes, respectively. It can be seen from Figure 16 that the shear stress of the side walls gradually increased with the backfill construction. The reason for this phenomenon is that with the backfill construction, the earthwork on both sides of the utility tunnel increased, leading to increased earth pressure on the main structure of the utility tunnel. Meanwhile, it can also be seen from Figure 16 that, for a certain construction stage, the shear stress of the side walls initially increased, then decreased, and finally increased with increasing distance from position 1. Therefore, the distribution and layout of the reinforcement in the side wall should be taken into

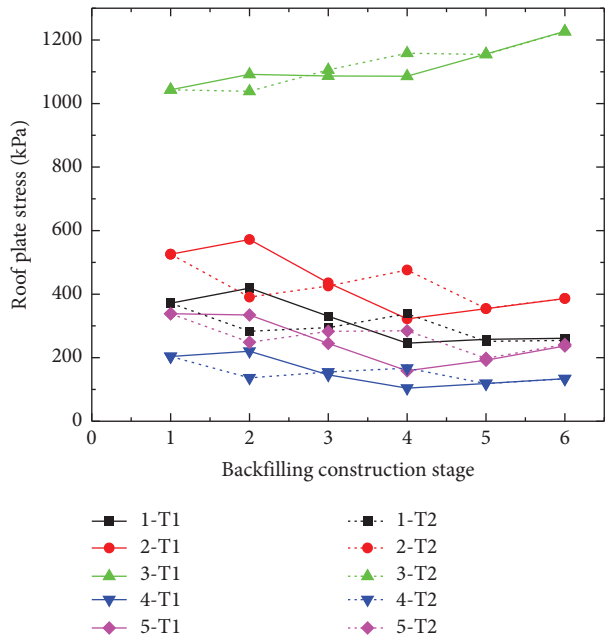

Figure 18: The stress of the roof in the left-to-right backfilling mode.

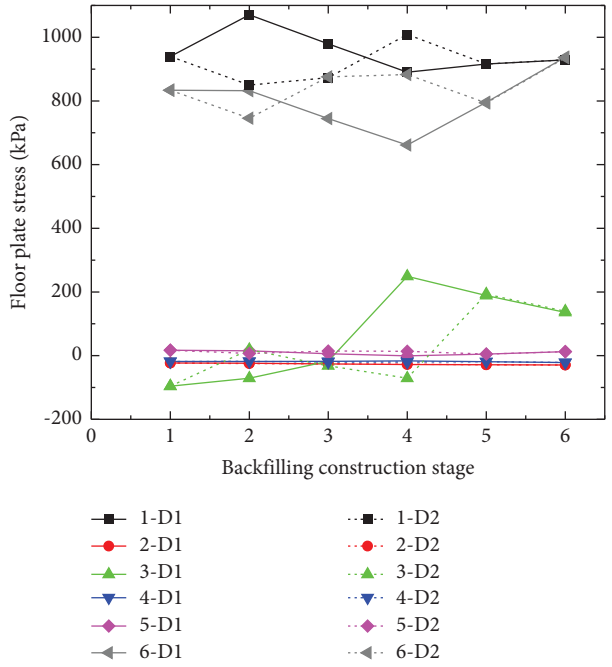

Figure 19: The stress of the floor in the left-to-right backfilling mode.

account in the construction process of the main structure of the utility tunnel. In addition, Figure 16 also shows that whether unilateral backfill or bilateral backfill occurred, the maximum shear stress of the side wall always appeared in either position 2 or position 5 of the left and right walls of the utility tunnel. Consequently, it is important to monitor these positions so as to prevent adverse conditions such as cracking failure of the side walls.

In a nutshell, in backfilling region 1, the unilateral backfill will cause obvious virtual displacement in the x direction of the side walls, while the bilateral backfill will not. At the same time, although the maximum shear stress of the left wall with a bilateral backfill scheme is much higher than that with a unilateral backfill scheme, there is no significant difference in the maximum shear stress of the right wall between the two schemes, which is almost equivalent to that

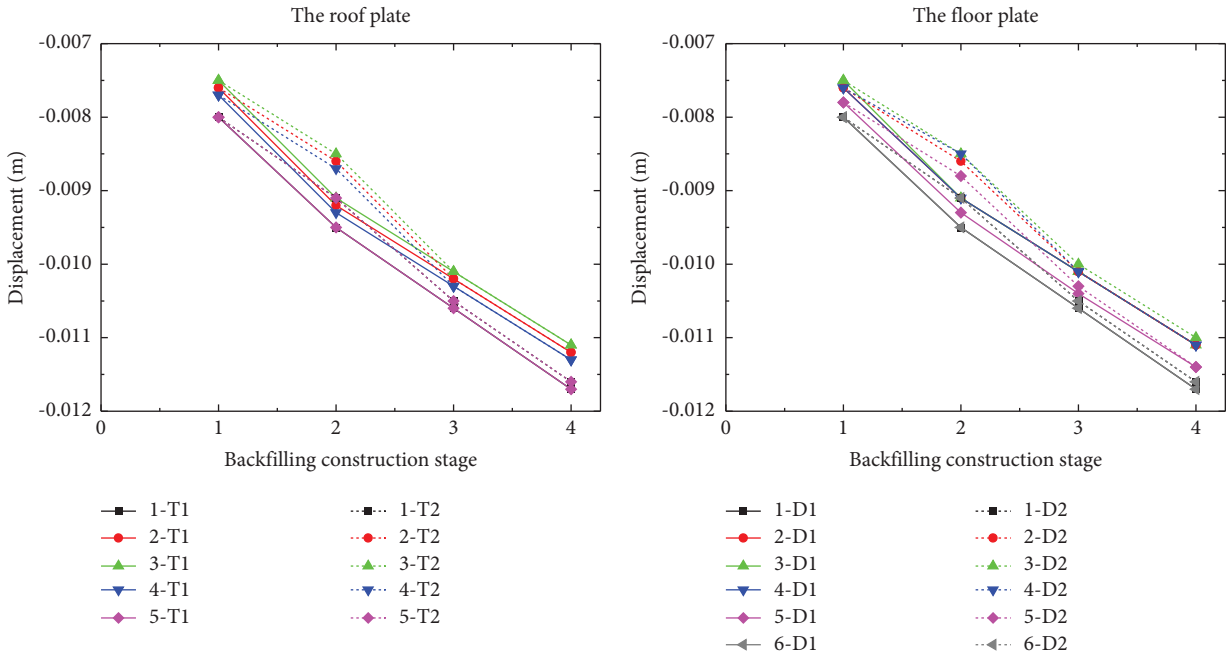

Figure 20: (Y)-direction virtual displacement of the roof/floor in the middle-to-side backfilling mode.

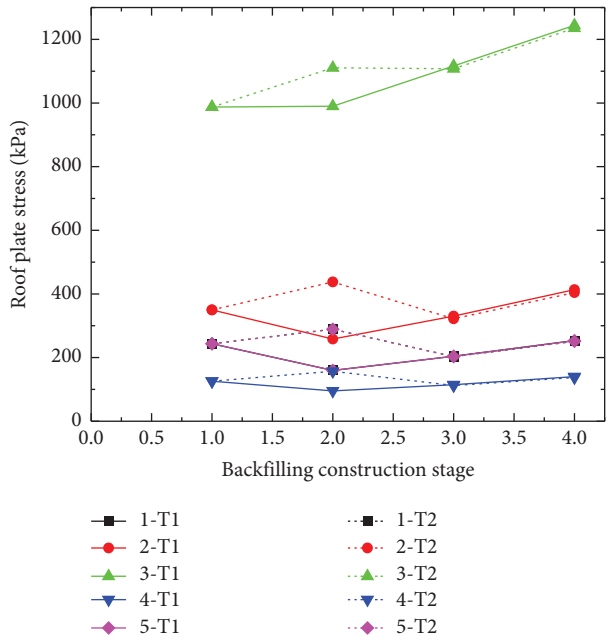

Figure 21: Stress of the roof in the middle-to-side backfilling mode.

of the left wall. In engineering practice, the side walls of the utility tunnel are all integrally poured at the site, i.e., the left wall is the same as the right wall. Thus, the bilateral backfill mode is most suitable for regions under the roof of the utility tunnel.

5.1.2. Influences of the Left-to-Right Backfilling Mode in Region 2. Figure 17 shows the variation law of displacement in the Y direction of the roof and floor of the utility tunnel when backfilling region 2 from the left to the right, where $x - T1$ (or $x - D1$) and $x - T2$ (or $x - D2$) represent the values read at position x of the roof (or floor) of the utility tunnel in Cases I and II. Obviously, with the backfill construction, the virtual displacements of the roof and floor of the utility tunnel in the opposite direction of y gradually increased. The reason for this variation is that with the increase in earthwork above the roof, the roof and floor are subjected to increasing earth pressure in the Y direction.

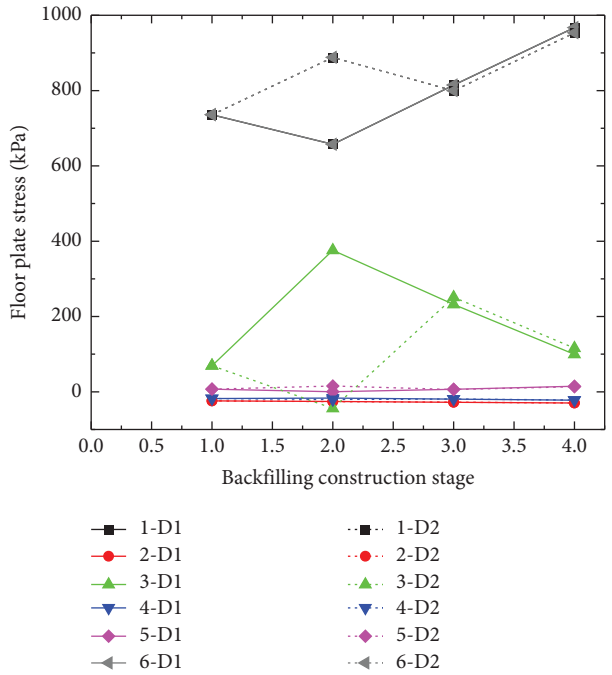

Figure 22: Stress of the floor in the middle-to-side backfilling mode.

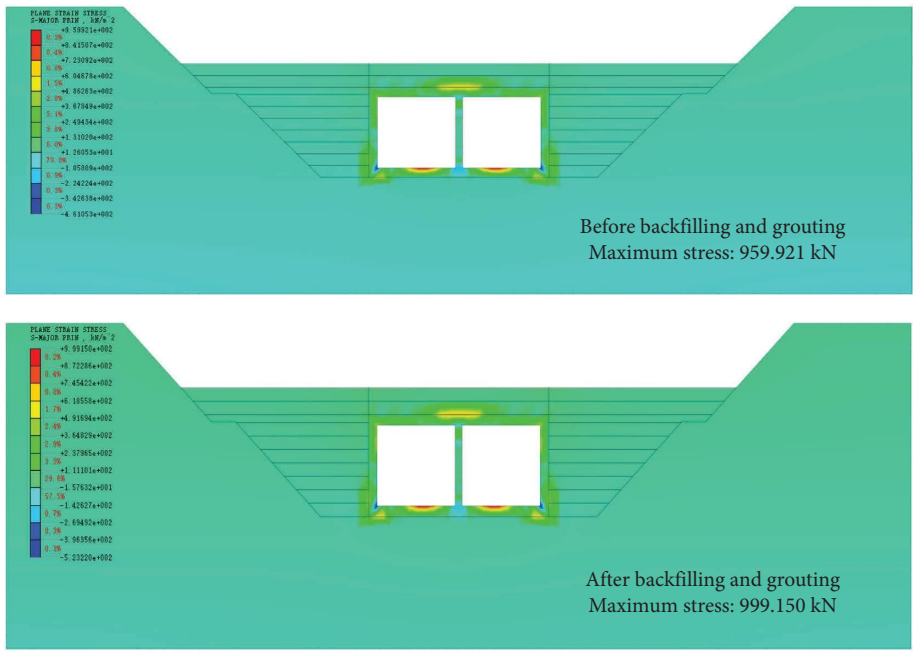

Figure 23: Overall stress changes of the model before and after grouting.

Figures 18 and 19 show the stress variation of the roof and floor when backfilling region 2 from left-to-right, respectively. It can be seen from Figure 18 that when Case I (or Case II) is adopted, the roof stress increases first, then decreases, and finally increases (or decreases first, then increases, and finally decreases) with the backfill construction. The reason for this rule is mainly that different backfill construction methods are adopted to make the soil stress distribution at different construction stages on the utility tunnel roof different. At the same time, it can also be found that under two different construction schemes, the stress in the middle position of the roof of the utility tunnel is the largest. Therefore, the center of the roof should be reinforced during the construction of the main structure of the utility tunnel. From Figure 19, it can be seen that the stresses generated in the interested positions are basically less than 200 kPa except for the corner positions on both sides of the bottom plate. The reason for this phenomenon is that tip

Figure 24: Stress changes of utility tunnel before and after backfill grouting.

stress effect was produced in the corners on both sides of the bottom plate. Therefore, in practical engineering, measures should be taken to avoid the stress concentration at the tip, such as replacing a right angle with a flat one. Meanwhile, it is conspicuous that the stress values of the roof and floor of the utility tunnel after backfilling were equal. For the roof, the stress value immediately after backfilling is the maximum in the whole backfilling process. However, for the floor, the maximum stress value appeared in the second stage. The reason for this situation is that different backfill construction schemes cause different earth pressures in the utility tunnel, displaying new stress distributions and combinations.

In summary, when backfilling region 2 in the left-to-right mode, there was a trivial difference in the displacements of the roof and floor, but the maximum stress value of the floor will be smaller if Case II is adopted.

5.1.3. Influences of the Middle-to-Side Backfilling Mode in Region 2. Figure 20 shows the displacement variation law in the Y direction of the roof and floor when backfilling region 2 in the middle-to-side mode. It can be seen from Figure 20 that with the backfill construction, the vertical pressures on the roof and floor were increasing, and the displacements in the Y direction were gradually increasing. The reason for this phenomenon is that the earthwork on the roof increased. At the same time, from Figure 20, it can also be found that, before stage 3, Case II led to smaller vertical displacements of the roof and floor. The reason for this change is that two different cases caused different distributions of earth pressure in the utility tunnel.

Figures 21 and 22 show the stress variation of the roof and floor when backfilling region 2 in the middle-to-side mode, respectively. Although the stress value and variation law were different in the two cases, the final results were the same. In addition, it can also be seen from Figures 21 and 22 that the maximum stress values of the roof and floor were after the completion of the utility tunnel backfill.

5.2. Grouting. Figures 23 and 24 are the stress nephograms of the model and the utility tunnel structure alone, before and after grouting. Figure 23 shows that the maximum stress increased by about 40 kN after backfill grouting. The reason for this situation is that after grouting, the gravity of the filling increased. As the backfill in both regions was compacted and grouted, the earth pressure on the main structure of the utility tunnel increased. In addition, since the strength parameters of the soil after grouting were greatly improved, as shown in Table 2, the numerical simulation results indicate that the proposed backfilling construction method is feasible. It can be seen from Figure 24 that the maximum and minimum stress values of the utility tunnel increased after

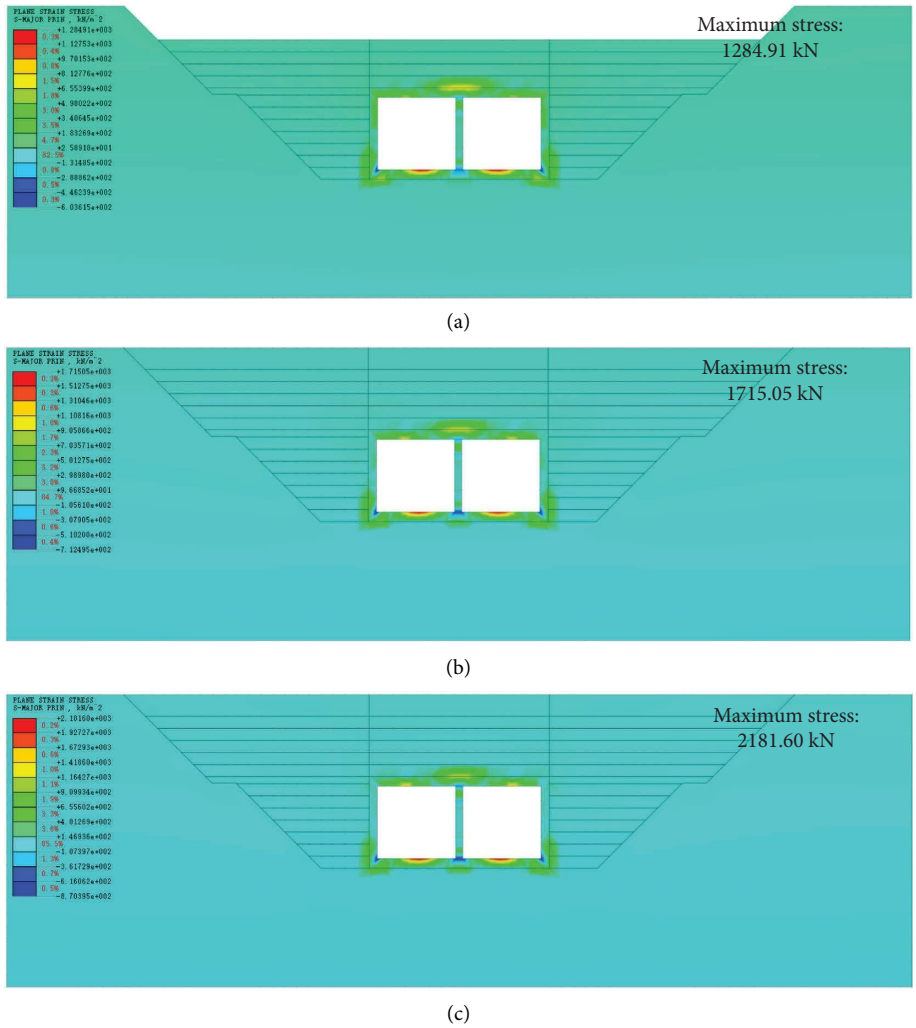

Figure 25: Change of backfilling stress of roadbed and water-stable layer. (a) Road base backfill. (b) Backfilling of water-stable pavement. (c) Consider the effect of river pressure.

grouting, but the positions where the maximum and minimum stress values appeared did not change significantly, viz., the maximum value appeared near the center of the roof, while the minimum value appeared near the corner of the floor. Therefore, in the design and construction of the main structure of the utility tunnel, the center of the roof and the corners of the floor should be reinforced.

5.3. Construction of the Subgrade and Water-Stable Pavement. Figures 25 and 26 are the stress nephograms of the model and the main structure of the utility tunnel during the backfilling process of the subgrade and water-stable layer pavement. Combined with Figures 23 and 25, it can be seen that after grouting is completed, the stress in the model increased by 285.76 kN after backfilling the road base and by 430.14 kN after backfilling the water-stable layer. Considering the effect of the water pressure of the 2.5 m deep river, the main structural stress increased by 466.55 kN. It can be seen from Figure 26 that the position of the maximum stress and minimum stress of the main structure of the utility tunnel did not change in the backfill of subgrade and water-stable pavement, which was basically consistent with the position of the maximum stress and minimum stress before and after the backfill grouting of the utility tunnel. However, it is necessary to consider the effect of overlying water pressure on the underground utility tunnel across the river. Therefore, after considering the river water pressure, the maximum stress position of the main structure of the utility tunnel changed from the central area of the roof to the central area of the floor. The reason for this situation is that water pressure acted not only on the excavation section of the foundation pit but also on the whole contact surface with the river, and thus the stress redistribution occurred. In summary, in the construction design of the main structure of the utility tunnel, attention should be paid to the centers of the roof and cabin and the floor's corners. Measures such as setting the armpit area, the reinforcement area, and foot protection can be adopted.

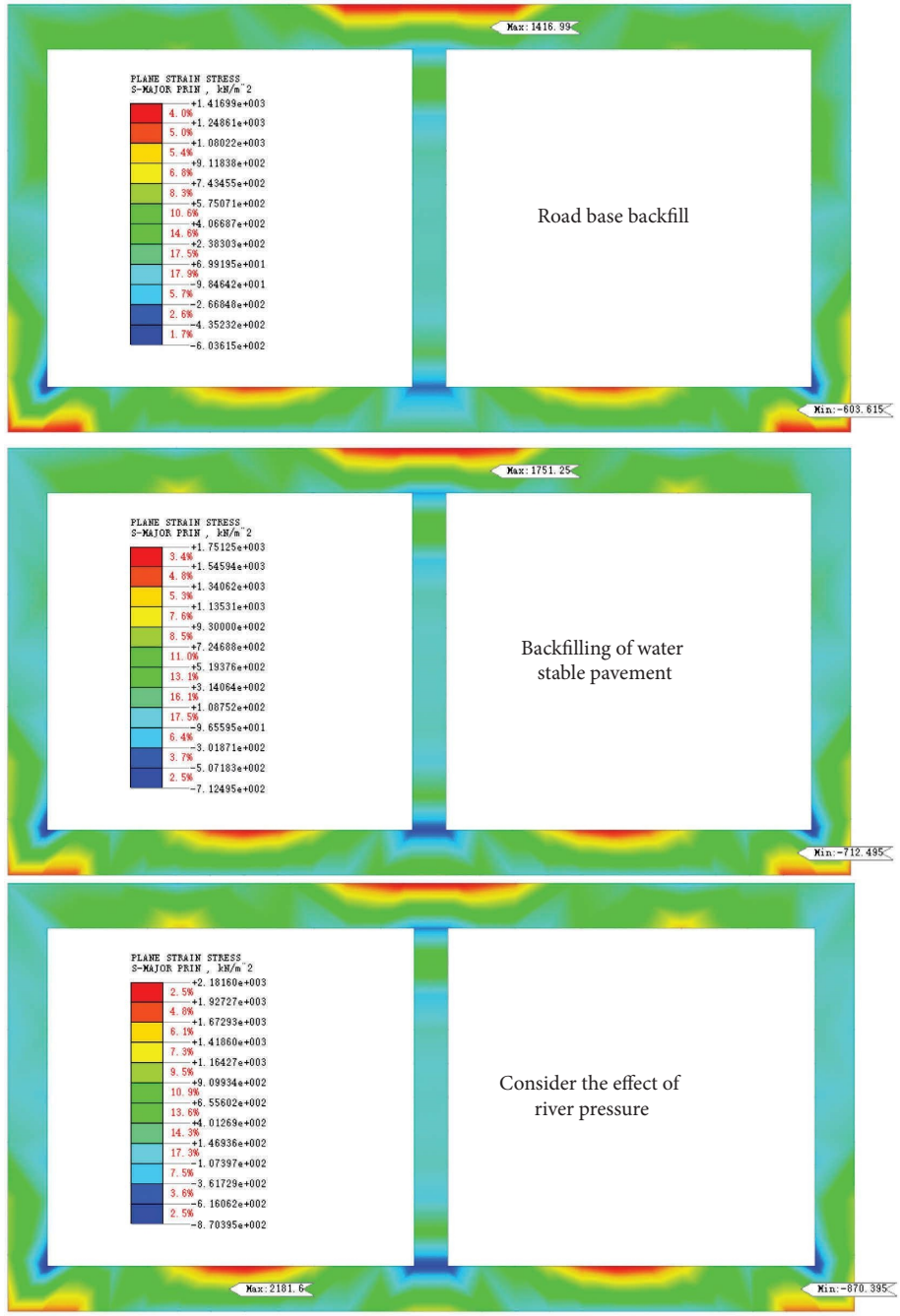

Figure 26: Stress variation of the utility tunnel in the backfilling of the roadbed and water-stable layer.

6. Conclusions

(1) In the process of unilateral backfill, the lateral wall displacement of the utility tunnel first increased and then decreased with the increase of backfill soil, and the maximum displacement always occurs upon finishing backfilling the left (or right) side of the utility tunnel.

(2) The shear stress of the side wall of the utility tunnel increased gradually with the backfill construction, no matter whether the backfill process was carried out in a unilateral or bilateral manner.

(3) Within 1 m above the top of the utility tunnel, the stress and displacement values of the utility tunnel were free from the effects of the backfill construction method.

(4) In the construction process of utility tunnel backfill, the construction scheme of bilateral backfill under the roof of the utility tunnel is the best.

(5) The unilateral backfilling mode is optimal for region 1, while any mode with Case II is the best for regions 2.

Data Availability

All data, models, or code generated or used during the study are available from the corresponding author by request.

Conflicts of Interest

The authors declare that they have no conflicts of interest.

Acknowledgments

This research was partially supported by the National Natural Science Foundation of China (grant no. 41807232).

References

[1] M. Sharifzadeh, F. Kolivand, M. Ghorbani, and S. Yasrobi, "Design of sequential excavation method for large span urban tunnels in soft ground – niayesh tunnel," *Tunnelling and Underground Space Technology*, vol. 35, pp. 178–188, 2013.

[2] Y. Luo, J. Chen, Y. Chen, P. Diao, and X. Qiao, "Longitudinal deformation profile of a tunnel in weak rock mass by using the back analysis method," *Tunnelling and Underground Space Technology*, vol. 71, pp. 478–493, 2018.

[3] L. Wang, A. Zhou, Y. Xu, and X. Xia, "Consolidation of partially saturated ground improved by impervious column inclusion: governing equations and semi-analytical solutions," *Journal of Rock Mechanics and Geotechnical Engineering*, vol. 14, no. 3, pp. 837–850, 2022.

[4] B. Wu, M. Lu, W. Huang, Y. Lan, Y. Wu, and Z. Huang, "A case study on the construction optimization decision scheme of urban subway tunnel based on the TOPSIS method," *KSCE Journal of Civil Engineering*, vol. 24, no. 11, pp. 3488–3500, 2020.

[5] Y. Wang, K. Feng, and W. Lu, "An environmental assessment and optimization method for contractors," *Journal of Cleaner Production*, vol. 142, pp. 1877–1891, 2017.

[6] C. Hu and S. Zhang, "Study on BIM technology application in the whole life cycle of the utility tunnel," in *Proceedings of the 2019 International Symposium for Intelligent Transportation and Smart City*, pp. 277–285, Shanghai , China, May 2019.

[7] Y. Zheng and Z. Shicheng, "Parametric modeling and application of tunnel based on BIM," *International Journal on Interactive Design and Manufacturing*, pp. 1–8, 2022.

[8] H. Liu, P. Li, and J. Liu, "Numerical investigation of underlying tunnel heave during a new tunnel construction," *Tunnelling and Underground Space Technology*, vol. 26, no. 2, pp. 276–283, 2011.

[9] A. Morovatdar, M. Palassi, and R. S. Ashtiani, "Effect of pipe characteristics in umbrella arch method on controlling tunneling-induced settlements in soft grounds," *Journal of Rock Mechanics and Geotechnical Engineering*, vol. 12, no. 5, pp. 984–1000, 2020.

[10] Y. Zhao, H. He, and P. Li, "Key techniques for the construction of high-speed railway large-section loess tunnels," *Engineering*, vol. 4, no. 2, pp. 254–259, 2018.

[11] J. Li, "Key technologies and applications of the design and manufacturing of non-circular TBMs," *Engineering*, vol. 3, no. 6, pp. 905–914, 2017.

[12] Y. L. Chen, R. Azzam, T. M. Fernandez-Steeger, and L. Li, "Studies on construction pre-control of a connection aisle between two neighbouring tunnels in shanghai by means of 3D FEM, neural networks and fuzzy logic," *Geotechnical & Geological Engineering*, vol. 27, no. 1, pp. 155–167, 2009.

[13] B. Lu, J. Dong, W. Zhao et al., "Novel pipe-roof method for a super shallow buried and large-span metro underground station," *Underground Space*, vol. 7, no. 1, pp. 134–150, 2022.

[14] X. Miao, M. Zhang, Y. Wang, and B. Liang, "Mechanical characteristics and optimum design of SMW construction method for a comprehensive pipe gallery in a water-rich weak stratum," *Journal of Highway and Transportation Research and Development*, vol. 14, no. 4, pp. 59–69, 2020.

[15] H. Che, L. Tong, S. Liu, and Q. Yang, "Field investigation on the mechanical performance of corrugated steel utility tunnel (CSUT)," *Journal of Constructional Steel Research*, vol. 183, Article ID 106693, 2021.

[16] Q. Sun, J. Zhang, Q. Zhang, and H. Yan, "A case study of mining-induced impacts on the stability of multi-tunnels with the backfill mining method and controlling strategies," *Environmental Earth Sciences*, vol. 77, no. 6, pp. 234–313, 2018.

[17] Y. Wang, J. Wang, and F. Peng, "Study on the characteristics of surrounding rock and design of backfill material parameters for tunnels passing through giant caverns and underground rivers," *Applied Sciences*, vol. 12, no. 8, p. 3906, 2022.

[18] B. Yao, L. Du, and L. Wan, "Research on the key technology of backfilling the fluid cement pit of integrated pipe corridor," *Jiangxi Building Materials*, no. 9, pp. 244-245, 2021, (in Chinese).